Quantum transport in the coupled multichannel case

1993 J. Phys.: Condens. Matter 5 5019

(http://iopscience.iop.org/0953-8984/5/28/016)

J. Phys.: Condens. Matter 5 (1993) 5019–5026. Printed in the UK

Quantum transport in the coupled multichannel case

Jianmin Mao, Qi Huang, Wenqing Cheng and Junming Zhou
CCAST (World Laboratory), PO Box 8730, Beijing 100080, People's Republic of China and Institute of Physics, Academia Sinica, PO Box 603-36, Beijing 100080, People's Republic of China†

Received 4 January 1993, in final form 5 March 1993

Abstract. We give a phenomenological formula for interedge channel scattering (IES) in the multichannel case. The equilibrium length over which the population of different channels is equilibrated is extracted from the experiments. The four-terminal resistances for the transport through edge and bulk currents are calculated in real conductors by taking into account scattering which equilibrates different transport channels. Negative resistances are found in the simulation. This makes it clear that the coexistence of bulk and edge states, together with interedge scattering, is the origin of the negative resistances observed in a variety of samples.

1. Introduction

Since the pioneering work of von Klitzing *et al* [1] the quantum Hall effect (QHE) has presented a major challenge. The QHE is usually treated by invoking the presence of localized states [2]. However, the recently developed Landauer–Büttiker formalism [3–9] has proved useful in understanding two-dimensional electron systems in the QHE regime, especially the anomalous QHE in high magnetic field. The edge channel picture rests on the idea that the current is carried by the edge states which are located at the boundaries of the sample. These channels carry a current $I = (2e/h)\Delta\mu$ because of the cancellation of one-dimensional group velocity and state density; here $\Delta\mu$ is the chemical potential difference between the two edge channels on the opposite sides of the sample. Under the equilibrium condition, the channels are equally populated according to the chemical potential of the contact and the normal QHE is obtained. However, for the non-equilibrium transport, i.e. incomplete occupation of one or more edge channels, deviation from ideal quantization can be detected.

Many experiments which aim at studying the anomalous Hall and longitudinal resistances have appeared. The results can be well understood in the edge channel picture by addressing the role of contacts and the long equilibrium length between edge states [10–14]. In the usual experiments, non-equilibrium is achieved by gate-induced backscattering or by selective population and detection of edge states with the help of quantum point contacts, and the geometric length is smaller than the equilibrium length l_{eq}, so that the effect of interedge channel scattering can be neglected. However, when l_{eq} is comparable with/longer than the Hall bar length, the effect of interedge channel scattering (IES) on the evolution of chemical potentials of the channels may be important. Theoretical work on IES by considering impurity, disorder and phonon scattering does show suppression of IES in a high magnetic field [15–17]. The IES depends on boundary potential. The commonly used parabolic potential cannot explain the extremely long l_{eq} between topmost and lower

† Mailing address.

0953-8984/93/285019+08$07.50

channels, because it gives equal spatial separation between the edge channels. The soft boundary is required, and it can explain the resistance anomalies in a ballistic junction [18]. Recent experiments using light illumination showed that a steeper boundary could reduce l_{eq} [19]. Therefore, to study the measured resistances in a real conductor, it is useful to extract l_{eq} from experiments.

The non-equilibrium population can be realized when the topmost channel undergoes backscattering. This is the case in the Shubnikov–de Haas (SdH) oscillation regime. The SdH oscillations appear when the Fermi energy level of the two-dimensional electron system coincides with the bulk Landau level. It is believed that in this situation the topmost channel, which is localized at the sample boundary, will spread into the bulk. Backscattering between the topmost channels on opposite sites of the sample occurs. At the same time the topmost channel decouples from the other edge states due to a decrease in the scattering rate between them [12]. Backscattering is also possible in very narrow channels when there is overlap of edge states on opposites or by tunnelling via impurity or disorder, especially for devices with low mobility and in very narrow Hall bars [20,21]. In the above situation, edge and bulk states can both contribute to the transport. This may be the origin of the negative local and non-local four-terminal resistance (LFTR, NFTR) found experimentally. The non-ideal contacts which have different transmission probabilities for incident and outgoing channels may also contribute to this [22,23]. In a usual experimental sample, both these effects can cause anomalous resistances. At very low temperature, the inelastic scattering length will be large. Strictly speaking, all the probes are non-ideal, i.e., electrons which enter the contacts cannot relax their energies completely, and anomalous temperature-dependent resistances can be observed [21]. Backscattering can be modelled by using a barrier which lets the topmost channel transmit partially and other channels transmit freely [13,24]. In this paper, we report the calculated four-terminal resistance (FTRs) in the transport through edge and bulk currents by taking into account IES. We will show that negative NFTR and even LFTR are possible by taking IES into account. Generally, backscattering reduces the chemical potential of the topmost channel at the higher-energy site, while IES will cause an increase of the chemical potential. These two competing factors make it possible to explain the anomalous chemical potential distribution among contacts and to obtain negative resistances. In section 2 we will build up the formulae which describe the evolution of the chemical potentials due to IES, and deduce the scattering length from the experiment in a three-channel case. The theoretical approach for the regime with edge and bulk states is arranged in section 3, and in section 4 we will give the calculated results for real conductors. As a conclusion, a brief summary is given at the end of the paper.

2. Relationship between interedge scattering length and chemical potentials

The one-dimensional edge channels which are located at the boundaries of the sample in a quantizing magnetic field will circulate along the periphery and enter the contact where energy relaxation takes place. If they are equally populated, the chemical potentials will remain unchanged during travelling. When there is some difference at the beginning, there will be exchange of electrons between them due to possible scattering from impurities, disorders, roughness and phonons. The IES length is proportional to $\exp(\Delta x^2/2l_B^2)$ [15], where $l_B = (\hbar/eB)^{1/2}$ is the magnetic length and Δx is the spatial separation between neighbouring edge channels. The larger Δx the longer is l_{eq}. So we will only consider IES in nearest-neighbour channels.

Suppose that there are n channels with chemical potentials $\mu_{10}, \ldots, \mu_{i0}, \ldots, \mu_{n0}$ at a given position, say $y_0 = 0$. The electrons travel along the boundaries to a position y, the

chemical potentials become $\mu_1, \ldots, \mu_i, \ldots, \mu_n$. We may use the differential equation to find the evolution†

$$\frac{\partial \mu_i}{\partial y} = -(\mu_i - \mu_{i-1})/l_{i-1,i} - (\mu_i - \mu_{i+1})/l_{i,i+1} \tag{1}$$

where $l_{i-1,i}$ ($i = 1, 2, ..., n$) is the equilibrium scattering length between the ith and $(i-1)$th channel. The above equation can be solved when the chemical potentials at $y_0 = 0$ are given. For simplicity, we will give the analytical forms in the three-channel case,

$$\begin{aligned}
\mu_1(y) &= \alpha + \beta\lambda_2' e^{(\lambda_2 y)} + \gamma\lambda_3' e^{(\lambda_3 y)} \\
\mu_2(y) &= \alpha + \beta e^{(\lambda_2 y)} + \gamma e^{(\lambda_3 y)} \\
\mu_3(y) &= \alpha + \beta\lambda_2'' e^{(\lambda_2 y)} + \gamma\lambda_3'' e^{(\lambda_3 y)}
\end{aligned} \tag{2}$$

where α, β and γ are functions of l_{12}, l_{23} and μ_{10}, μ_{20}, μ_{30}; while λ_2, λ_2', λ_2'', λ_3, λ_3', λ_3'' are the functions of l_{12} and l_{23}.

Most experiments have focused on the two-channel case or cannot be compared with theory quantitatively. The only experiment which gave the data in detail for the three-channel case was reported in [12]. Here we will briefly describe that experiment. Alphenaar *et al* used two point contacts to realize selective population and detection, and measured the Hall resistance. (The separation between the two point contacts is not so long that deviations from the exact value can be detected in the experiment.) It is easy to express the Hall resistance R_H based upon the Landauer–Büttiker formalism as $R_H = (\sum_i T_i\mu_i)/TeJ$. Here μ_i is the chemical potential and T_i is the transmission probability of the ith channel incident on the non-ideal voltage probe. $T = \sum_i T_i$ is the total transmission probability of the three incident channels. If the non-ideal current probe only populates the first channel, i.e. $\mu_{10} = (h/2e)J$, $\mu_{20} = \mu_{30} = 0$, and let the non-ideal voltage contact probe the first or the first two channels, from the measured resistances we obtain $\mu_1 = 0.48(h/2e)J$, $\mu_2 = 0.44(h/2e)J$ and $\mu_3 = 0.08(h/2e)J$ for a separation of 80 μm. Data are also deduced for separation distances of 130 μm and 210 μm at 0.45 K. Then we extract $l_{12} = 39.6$ μm and $l_{23} = 319$ μm by the method of minimum squares. These parameters are consistent with the theoretical calculation [16, 17]. It should be pointed out that the equilibrium length defined by us is as twice as that of [16]. Komiyama *et al* only considered the two-channel case and used a single equation to link the difference of the chemical potentials between two channels with the equilibrium length. The equilibrium length is reduced drastically as the temperature increases, e.g. l_{23} from 319 μm at 0.45 K to 25 μm at 4.2 K, while l_{12} changes more slowly, from 39.6 μm to 19 μm.

3. Theoretical approach for transport through edge and bulk states

In the SdH regime, the topmost channel suffers backscattering which is similar to putting a barrier in the Hall bar. The electrons in the topmost channel pass the barrier with transmission probability t, and the transmission probability in each section is related to an intensive parameter ρ_{xx}^{N+1}, i.e. the resistivity of the topmost channel, by the Landauer formula [13]. If we divide each section into many segments, each segment has the same ratio

† The current carried by the ith channel is $(2e/h)\mu_i$. The change in the number of electrons in the ith channel is accompanied by a change in the current. Then the change of the chemical potential is proportional to the change in the number of electrons. The formulae is easily obtained by defining the IES length.

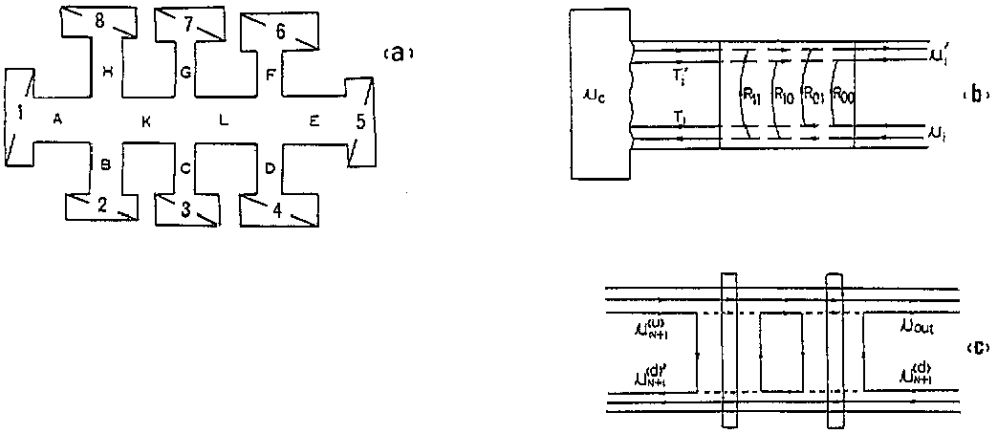

Figure 1. (*a*) Schematic of an eight-probe Hall measurement and ten sections in which the topmost channel suffers backscattering. (*b*) The reservoir and a barrier with transmission and reflection probabilities. (*c*) Two barriers in a section with no contact attached and the transmission of the topmost channel.

of length to width. Then each segment acting as a barrier will have the same transmission probability for the topmost channel. In other words, here t is an intensive parameter.

For the case with $N+1$ channels, only the $N+1$th is backscattered. Following Komiyama and by using current conservation and the Landauer–Büttiker formalism, two equations which relate the chemical potentials of the outgoing channels to those of the incident channels can be written (with an ideal contact attached, see figure 1(*b*)) as [11, 24]

$$\mu_i' = \frac{1}{N+t+(n_j-1)Nr}\left[\left[1+(n_j-1)r\right]\sum\mu_i + t\mu_{N+1} + \left[1+(n_j-1)r\right]\frac{h}{2e}J\right] \qquad (i=1,2,\ldots,N)$$
$$\mu_{N+1}' = \frac{1}{N+t+(n_j-1)Nr}\left[t\sum\mu_i + (t+n_jNr)\mu_{N+1} + t\frac{h}{2e}J\right] \qquad (3)$$

where μ_i, μ_i' are the chemical potentials of the ith incident and outgoing channels, and μ_{N+1}, μ_{N+1}' are the incident and outgoing chemical potentials for the topmost channel. $\sum\mu_i$ represents the sum of chemical potentials of all the N lower incident channels, t and r (=1−t) are the transmission and reflection probabilities for each barrier, and n_j is the number of the barriers in the jth section. (In the following calculations, we have chosen $n_j = L_j/W_j$. Here L_j, W_j are the length and width in the jth section.) Obviously, the chemical potential of the contact is equal to that of the lower N channels for the reason that the lower N channels transmit the barrier freely and the contact is ideal. A typical Hall measurement is like figure 1(*a*). Ten sections where backscattering happens should be considered. We will denote them as A, B, C, D, E, F, G, H, K and L. The above two equations can correctly describe the chemical potentials of the ten sections except for K and L. In regions K and L no contacts are attached as shown in figure 1(*c*). Current conservation requires [24]

$$\mu_{out} = \left[n_k r\mu_{N+1}^{(d)'} + (t-n_k r)\mu_{N+1}^{(u)}\right]/t \qquad (4)$$

where n_k is the number of barriers in section K. $\mu_{N+1}^{(d)'}$ and $\mu_{N+1}^{(u)}$ are the chemical potentials of the N+1th channel for the outgoing one at the lower side and for the incident one

at the upper side. All the above three equations together with equations (1) and (2) are mathematically complete and can be solved to obtain potentials of any contacts in any configuration, and hence resistances and energy exchanges between bulk and edge currents [24].

4. Calculations of local and non-local resistances

Recent experiments revealed many novel phenomena for the transport in low-dimensional electron systems. Among these are the anomalous FTRs in strong magnetic fields. It is believed that these phenomena appear when there is co-existence of bulk and edge states. By using a non-ideal contact, Takaoaka *et al* found that the negative FTRs were produced by unequal population and transmission probability from the contact [22, 23]. However, negative resistances were also found in narrow systems with ideal contacts. To our knowledge, there is no quantitative explanation for this problem to date. Below we will show that transport through bulk and edge states as well as IES can explain it well.

Let us denote an FTR in a multiprobe sample by $R_{ij,kl} = (\mu_k - \mu_l)/eJ$, where $\mu_k - \mu_l$ is the chemical potential difference between contacts k and l, and the current is transmitted from contacts i to j. Though a number of papers have been published on this aspect, only a few of them are available for comparison with the theory. Some of them have not given the geometrical length or cannot know the IES length. Our calculations are focused on [13] and [22].

4.1. Local four-terminal resistance

The Hall bar configuration used in [13] has eight probes (see figure 1(*a*)). Calculations by means of a decoupled model [13, 24], i.e. the bulk channel is totally decoupled from the edge states, showed that the local resistances $R_{15,76}$ and $R_{15,34}$ as a function of $R_H = R_{15,37}$ are basically consistent with experiment, but the peak values are smaller than the experiment. The mobility of the sample is 1.2×10^6 cm^2 V^{-1} s^{-1} which is 2.4 times the value given in [12]. The other experimental parameters are the same. At a temperature of 0.45 K, impurity scattering dominates the IES. We may reasonably take l_{eq} to be 2.4 times that of [12], that is $l_{12} = 95$ μm, $l_{23} = 765.6$ μm. Our calculations are based on these data. (In fact, the relationship between the IES length and the mobility of the sample is unknown.)

Figure 2 gives the curves of $R_{15,76}$, $R_{15,34}$ versus $R_{15,37}$ obtained with the decoupled model and with the IES. Now, we can see that the calculated peak of $R_{15,76}$ obtained with IES is bigger than that obtained with the decoupled model, and is nearly equal to that of experiment. (The peak of $R_{15,76}$ is 10.7 for the experiment, 10.6 for the calculation which includes IES and 8.8 in the decoupled model.) We may explain it in this way: the topmost channel suffers backscattering, and non-equilibrium between it and the lower channels occurs. Some electrons in the lower channels will participate in the backscattering via IES through the topmost channel. It should be mentioned that in the calculation we have changed the IES length between the topmost channel and the second one to l_{23}/t^{σ}. Here l_{23} is the IES length in the Hall plateau region where no backscattering takes place. When SdH oscillations emerge, the topmost channel will spread to the bulk of the sample depending on the magnetic field (or transmission t) and causes a decrease in the scattering rate between it and the lower edge channels. Therefore, the equilibration length is changed and depends on the transmission probability. In the calculation $\sigma = 8$ is chosen, which can well describe the larger-t regime, but fails in the smaller-t regime. In the smaller-t

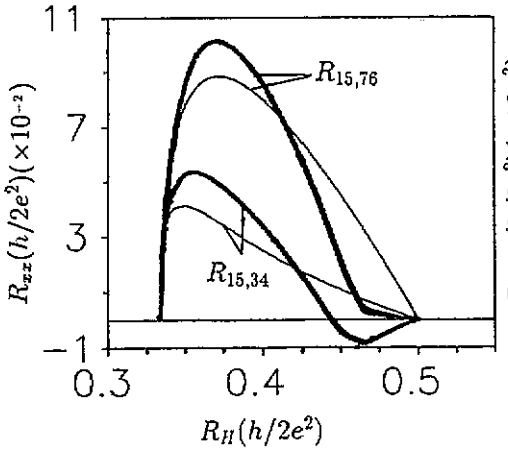

Figure 2. Longitudinal resistances of $R_{15,76}$, $R_{15,34}$ versus Hall resistance $R_{15,37}$ with (bold curve) and without (fine curve) IES. Parameters are taken from [13].

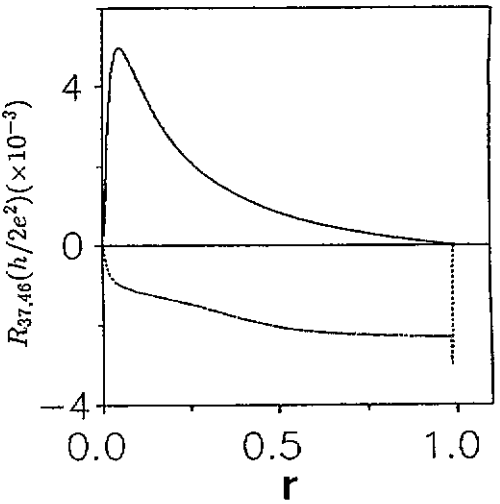

Figure 3. Non-local resistance of $R_{37,46}$ versus reflection probability r with (broken curve) and without (full curve) IES. Parameters are taken from [13].

regime (or higher-magnetic-field side), the topmost channel will be a bulk state throughout the sample†

An interesting result is the negative values of $R_{15,34}$ in the small-t regime. In this area, the topmost channel is strongly backscattered, while the IES is strongly dependent on the difference between the unequal chemical potentials of the channels. This results in more electrons being backscattered and lower potentials in the contact, such as contact 3. The negative resistance discussed here does not need inverted population of the channels as in [22] and [23].

4.2. Non-local four-terminal resistance

Non-local resistances are measured with the help of voltage probes that are far from the current path. Classically the resistances decay exponentially as $\exp(-L/W)$. Here L is the distance from the current path, W is the channel width. However, adiabatic transport can survive as long as 1 mm and NFTRs will be much bigger than the classical value. This demonstrates definitely the edge channel picture and suppression of the IES in high magnetic field. Negative FTRs have been found in GaAs/AlGaAs heterostructures and Si-MOSFETs in narrow systems, and the explanation remains unresolved [20–23].

We have calculated the NFTR seen in [13]. The NFTR is plotted against the reflection probability r in figure 3. For comparison, the NFTR in the decoupled model is also calculated. When the IES is taken into consideration, $R_{37,46}$ will be negative in the whole regime, with a maximum near to the larger-r side. This is not surprising, as was indicated above. In such a configuration, the separation of the voltage probes from the current pathway is long and L/W is larger, so that more electrons are backscattered in the section. This is enough to cause the chemical potential of contact 4 to be lower than that of contact 6. To confirm this, we have calculated the NFTR in a similar configuration which is found in [22], but

† This indicates that $\sigma = 8$ cannot well describe the coupling between the topmost channel and the lower channels in the whole SdH regime. We do not know whether a suitable $f_{(T)}$ exists. In fact, the extended bulk state in this regime is an open question.

with different geometrical parameters. The IES length is chosen to be the same as in [12], because the experiment was conducted under similar conditions and the mobility of the sample used is nearly equal. The results are shown in figure 4. In contrast, we have not found any negative values for $R_{46,37}$, or $R_{28,37}$, $R_{37,46}$, $R_{37,28}$ (not shown). The peak of $R_{46,37}$ approximates the experimental value, 37 Ω. We also found that the resistance with the IES is smaller than that with the decoupled model. This can be understood: the extremely large NFTR rests on the adiabatic transport. IES will weaken it; a decrease in resistance is expected. If IES were strong (short IES length) NFTR could approximate its classical value. This is verified by our calculation (not shown). We have set $l_{12} = 0.3$ μm, $l_{23} = 1.0$ μm and found that the NFTR will be nearly zero for a reflection probability of up to 0.7. However, there is a peak around 0.85, but its value is only about one third of that for weakly coupled channels.

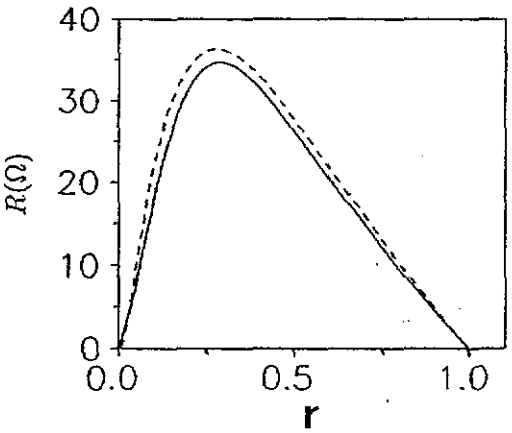

Figure 4. Non-local resistances of $R_{46,37}$ versus reflection probability t with (full curve) and without (broken curve) IES. Parameters are taken from [22].

By using a 'dirty' contact (high contact resistance), negative resistances were discovered in [22] and [23]. Our calculations do not show such negative LFTRs and NFTRs. Therefore, the negative resistances in these experiments are produced by non-ideal probes. The involved disordered contact is difficult to describe, i.e. the transmission and reflection probabilities for each incident and outgoing channel cannot be determined definitely. Anyway, if we can add the elastic scattering effect of a non-ideal probe to equation (3), negative resistances should be expected. The negative resistances in very narrow systems, we believe, also originate from the transport through coupled edge and bulk states. The observed characteristics of negative resistances in [20], which are nearly in antiphase relative to the positive resistances, and emerge at the beginning of the Hall plateau, can be understood from our calculations. Positive resistances appear in the smaller-r regime, while they are negative on the larger-r side, and peak at $r = 1$. (See figure 3. In the experiment, the antiphase effect is possible because the relationship between magnetic field B and reflection probability r is non-linear.) To quantitatively study the transport properties in narrow systems, it is necessary to take into account backscattering in the junction which is caused by geometric scattering, as the radius of curvature in this area is comparable with the magnetic length, and strong geometric scattering is possible [25].

5. A brief summary

In conclusion, we present a phenomenological formalism to describe the effect of IES on the change of chemical potentials of unequally populated channels, and extract the IES

length from experiments by using the method of least squares. The backscattering in the regime between Hall plateaus was modelled by barriers in each section of the Hall bar. The equations which govern the chemical potentials and the transmission probability for the topmost channel are built up. IES between nearest-neighbour channels is explicitly incorporated. The calculations of local and non-local resistances with an IES length deduced from the experiment in the three-channel case are in better agreement with that of the decoupled model. We are the first to report the negative resistances by calculation. Thus we demonstrate clearly that the negative resistances found in high magnetic fields are caused by the transport through coupled edge and bulk states. The FTRs are strongly dependent on the geometry of the Hall bar since the number of barriers is dependent on the length–width ratio, while the equilibration of the unequally populated channels due to IES depends on the electrons' travelling distance and this length relative to the IES length. Our method can be applied to disordered contacts and gate-induced backscattering as well as the backscattering in narrow systems.

References

[1] von Klitzing K, Dorda G and Pepper M 1980 *Phys. Rev. Lett.* **45** 494
[2] Prange R E and Girvin S M (ed) 1987 *The Quantum Hall Effect* (New York: Springer)
[3] Landauer R 1970 *IBM J. Res. Dev.* **1** 233; 1970 *Phil. Mag.* **21** 863
[4] Büttiker M 1988 *Phys. Rev.* B **38** 9375; 1986 *Phys. Rev. Lett.* **57** 1761; 1988 *IBM J. Res. Dev.* **32** 317
[5] Streda P, Kucera J and MacDonald A H 1987 *Phys. Rev. Lett.* **59** 1973
[6] Jain J K and Kivelson S A 1988 *Phys. Rev.* B **37** 4276; 1988 *Phys. Rev. Lett.* **60** 1542
[7] Sivan U, Imry Y and Hartzstein C 1989 *Phys. Rev.* B **39** 1242
[8] Peeters F M 1988 *Phys. Rev. Lett.* **61** 589
[9] Akera H and Ando T 1989 *Phys. Rev.* B **39** 5508
[10] van Wees B J, Willems E M M, Kouwenhoven L P, Harmans C J P M, Williamson J E, Foxon C T and Harris J J 1989 *Phys. Rev.* B **39** 8066
[11] Komiyama S, Hirai H, Sasa S and Hiyamizu S 1989 *Phys. Rev.* B **40** 12566
[12] Alphenaar B W, McEuen P L, Wheeler R G and Sacks R N 1990 *Phys. Rev. Lett.* **64** 677
[13] McEuen P L, Szafer A, Richter C A, Alphenaar B W, Jain J K, Stone A D, Wheeler R G and Sacks R N 1990 *Phys. Rev. Lett.* **64** 2062
[14] van Wees B J, Kouwenhoven L P, Willems E M M, Harmans C J P M, Mooij J E, van Houten H, Beenakker C W J, Williamson J G and Foxon C T 1991 *Phys. Rev.* B **43** 12431
[15] Martin T and Feng S 1990 *Phys. Rev. Lett.* **64** 1971
[16] Komiyama S, Hirai H, Ohsawa M, Matsuda Y, Sasa S and Fujii T 1992 *Phys. Rev.* B **45** 11085
[17] Maslov D L, Levinson Y B and Badalian S M 1992 *Phys. Rev.* B **46** 7002
[18] Geisel T, Ketzmerick R and Schedletzky O 1992 *Phys. Rev. Lett.* **69** 1680
[19] Müller G, Weiss D, von Klitzing K, Ploog K, Nickel H, Schlapp W and Lösch R 1992 *Phys. Rev. B* **46** 4336
[20] Ohata A and Toriumi A 1992 *Proc. 21st Int. Conf. on Physics of Semiconductors* (Singapore: World Scientific) at press
[21] Geim A K, Main P C, Beton P H, Streda P, Eaves L, Wilkinson C D W and Beaumont S P 1991 *Phys. Rev. Lett.* **67** 3014
[22] Takaoka S, Sawasaki T, Tsukagoshi K, Oto K, Murase K, Gamo K and Namba S 1991 *Solid State Commun.* **80** 571
[23] Oto K, Sawasaki T, Tsukagoshi K, Takaoka S, Murase K, Gamo K and Namba S 1992 *Proc. 21st Int. Conf. on Physics of Semiconductors* (Singapore: World Scientific) at press
[24] Mao J M, Zhou J M, Du Q H, Cheng W Q, Li Y K, Huang Y and Young G Z 1992 *Proc. 21st Int. Conf. on Physics of Semiconductors* (Singapore: World Scientific) at press
[25] Palacios J J and Tejedor C 1992 *Phys. Rev.* B **45** 9059